




Article

Case Study of Thermal Diagnostics of Single-Family House in Temperate Climate

Aleksandra Specjał , Aleksandra Lipczyńska , Maria Hurnik, Małgorzata Król ,
Agnieszka Palmowska and Zbigniew Popiołek

Department of Heating, Ventilation and Dust Removal Technology, Faculty of Energy and Environmental Engineering, Silesian University of Technology, Konarskiego 20, 44-100 Gliwice, Poland; aleksandra.lipczynska@polsl.pl (A.L.); maria.hurnik@polsl.pl (M.H.); Malgorzata.Krol@polsl.pl (M.K.); agnieszka.palmowska@polsl.pl (A.P.); zbigniew.popiolek@polsl.pl (Z.P.)

* Correspondence: aleksandra.specjal@polsl.pl; Tel.: +48-32-237-2556

Received: 30 October 2019; Accepted: 28 November 2019; Published: 29 November 2019



Abstract: Reduction of the primary energy consumption is a crucial challenge for the building sector due to economic and environmental issues. Substantial savings could be achieved within the household. In this paper, we investigate the energy performance of a single-family house located in the temperate climate. The assessment is based on the comprehensive thermal diagnostic of the building performed on-site and via computational analyses. The on-site measurements included diagnostics of the building envelope, heat source, heating and domestic hot water system, ventilation system, and indoor environmental quality. Analyses confirmed that the studied building, which was built in 2008, meets the legislation requirements for the primary energy usage at that time and nowadays. However, results show discrepancies between energy performance obtained through on-site measurements and computational methods following regulations. Partially, discrepancies are a result of differences on normative values and how the building is operated in practice. It is also showed how important the role in the assessment of energy consumption through measurements is played by the measurement period.

Keywords: thermal diagnostics; energy performance; case study; temperate climate

1. Introduction

The construction sector is the second largest consumer of energy worldwide [1,2]. Following the requirements of the European Union (EU), from 2021, the maximum annual building demand for non-renewable primary energy for heating, ventilation, cooling, domestic hot water (DHW) preparation, and lighting should not exceed 70 kWh/(m²·year) [3]. This means a significant reduction in energy consumption in residential buildings. Poland is gradually preparing for these changes. Nowadays, newly constructed single-family buildings have been required to achieve a primary energy consumption index for heating, ventilation, and DHW lower than 95 kWh/(m²·year) [4]. About 79% of the energy used in EU households is for space heating and DHW preparation [5]. Therefore, it is necessary to look for savings in these areas as most buildings (approximately 5 million) do not meet the stringent requirements for energy consumption.

To assess how much energy a building consumes and what is its primary energy consumption index for heating, ventilation, and DHW, computer simulations or on-site measurements should be made [6–10]. Sometimes, on-site studies are performed as a way of obtaining input data for computer calculations. Jermyn and Richman used building data collected through on-site measurements to create energy models in EnergyPlus. Then, they used these models for the development of retrofit strategies according to the brute force method [9]. Pellegrino et al. followed a similar approach [10].

They used on-site measurement to validate the building model created in EnergyPlus, on which they based their later analyses on how to reduce thermal discomfort of occupants and energy consumption. Comprehensive computer simulations are easier to perform compared to on-site measurements. However, the use of computer simulations methods involves the risk that the data assumed at the beginning of the calculations are incorrect. Unfortunately, there are additional discrepancies between the simulation results and the results of measurements involving energy consumption in buildings [11,12]. It is reported that these discrepancies result from differences between the real world and simulation inputs [13–15]. Although on-site tests are most often fragmentary and strictly connected to the duration of the measurements, they take into account the behavior of residents and weather changes. It is difficult to reflect the wide variety of human behavior in simulations, which often boils down to considerable simplifications in energy consumption determined by simulations comparing to results obtained by measurements. Another reason for discrepancies may be differences in the assumed efficiency of devices. The efficiency of devices, assumed in simulations based on documentation, does not coincide with the actual efficiency with which a specific device or the entire installation works.

On-site measurements should, therefore, provide more reliable information. However, such measurements are often difficult to carry out. Difficulties are related to getting to the right places in the installation where measuring points can be located. In a single-family house, internal installations are often hidden, which is required by the aesthetics of the rooms. On-site measurements can also cause discomfort for building users. Sometimes, some measurement procedures are impossible to take place at the studied location. The solution may be to use measuring devices permanently installed in the building, continuously measuring the consumption of, for example, water or gas. Furthermore, there are problems with selecting the right period of the year to perform such measurements. Selection of the measurement period is particularly important for buildings located in the temperate climate [16,17].

Knowing the need to reduce the consumption of non-renewable primary energy by 2021, in-depth analysis and on-site measurements are necessary. Such research has already been undertaken by scientists [18]. López-González et al. presented a methodology for evaluating the final energy consumption, primary energy consumption, and contribution by renewable energy in the residential sectors [19]. There is also extensive research covering energy consumption in 50 residential buildings. As part of this research, programs are being implemented that look for correlations between building users' habits and energy consumption [20]. While analyzing the structure of energy consumption in residential buildings in China, Zhao et al. noted the large variety [21]. This makes it necessary to implement various programs promoting energy saving affecting various areas of life. In Poland, the "Development of Thermal Diagnostics of Buildings" research project was carried out as a work package of "Integrated System for Reducing Energy Consumption in the Maintenance of Buildings"—a large strategic project financed by the Polish National Centre for Research and Development. The main goal of the research project was to develop and disseminate new tools for thermal diagnostics of various types of buildings. It covered analyses of single-family buildings, multi-family buildings, public buildings (school), and office buildings. The assessment of energy consumption was based on data characterizing the energy efficiency of heating, ventilation and air-conditioning (HVAC) and DHW systems, obtained through field experiments. Project results were presented in six volumes of the "Guide to thermal diagnostics of buildings". The individual volumes describe the methods for diagnosing the building's thermal insulation [22], diagnostic methods of heat sources [23], diagnostic methods of cooling sources and ventilation [24], diagnostic methods of indoor environment in buildings [25], comprehensive on-site thermal analysis of various buildings [26], and methodology for performing building energy certificate based on the measurements [27]. There were also several articles describing parts of the project and achieved results. The seasonal heat demand in buildings based on short measurement periods was presented in [28–30]. Indoor environmental conditions were analyzed focusing on the operative temperature and air quality [31,32]. The analysis of the building's insulation condition was examined in terms of determining seasonal heat consumption [33–35]. On-site diagnostics of mechanical ventilation systems and of cooling sources for air conditioning systems

in office buildings were also presented in [36,37]. The determination of seasonal energy demand for cooling based on short measurements was also shown [38]. On-site measurements of energy consumption for heating and DHW installations were presented in [39,40].

In this paper, we present results of energy assessment not yet published for a single-family house built in 2008. The building met then the energy consumption requirements for the needs of heating, ventilation and DHW systems. Compared to the previously published articles on energy consumption in residential buildings, our research focuses on one single-family house. The small, limited research space allowed us to perform very thorough on-site measurements and very accurate analysis of energy consumption. On-site measurements were made to check whether the examined single-family building meets, in practice, the primary energy consumption index for heating, ventilation, and DHW requirements that were set for the building constructed in 2008 [4]. Data collected during the energy diagnostics of the building and its installations were also applied to determine the energy performance of the object using two methods: First, analytical based on the performed on-site measurements of the heat consumption in the building; and second, computational, calculated in accordance with the Regulation [41]. Results show how important role in the assessment of energy consumption through measurements is played by the measurement period. Especially for building in a temperate climate according to the Koppen-Geiger climate classification [42], the selection of the season during which the measurements will be carried out is crucial.

2. Study Side

A comprehensive thermal diagnostics was performed in the detached two-story single-family house without a basement shown in Figure 1. The house was built in 2008 according to the technical requirements at that time. It is located in the southern region of Poland on the city outskirts, in the neighborhood of single-family houses.



Figure 1. View of the experimental house.

Heated building area of 185 m² includes a kitchen combined with living room, 3 bathrooms, 4 bedrooms, utility room, garage, and corridors. Three residents use the space.

2.1. Building Envelope

The examined building was constructed using the traditional technology. External and curtain walls are made of Porotherm ceramic blocks of 25 cm thick. The building is thermally insulated with the polystyrene with rendering (ETICS system). The thickness of the polystyrene layer is equal to 14 cm. The roof structure is wooden with mineral wool insulation of 24 cm placed between the rafters. Internal partition walls consist of brick blocks with a thickness of 11 cm. The ceiling over the first floor is constructed of prefabricated beams and hollow block slabs, while the attic ceiling is a wooden construction. The concrete ground floor, insulated with polystyrene, is covered with ceramic tiles.

2.2. Heat Source

The analyzed building uses multi-source heat. The central element of the heating system is a water heat buffer with the capacity of 550 L, which is supplied by three elements: (1) A fireplace with a water jacket (with a built-in heat exchanger), (2) a set of 4 vacuum-tube solar collectors, and (3) an electric boiler (power 1–18 kW). The simplified system diagram is shown in Figure 2. During the heating season, the heat for the buffer comes mainly from the fireplace (if used) or the electric boiler, and from solar collectors on days with sufficient solar radiation. Outside the heating season and in summer, the solar collectors are the primary heat source supported by the electrical boiler on days with low solar radiation. The heat is accumulated in a multi-layer buffer, in which the highest zone is used as a water storage for heating of DHW, and lower zones (with lower water temperature) for a hydronic floor heating. The heater (hot water tank) for the DHW is placed inside the heat buffer. Solar collectors are located on the roof with a 45° slope and a surface azimuth of 20° (South-Southwest). The operation of the solar collector system is regulated by a controller that adjusts the rotational speed of solar circuit pump depending on the temperature difference in the solar collector and in the heat buffer. The heat source is in a good technical condition and is properly used.

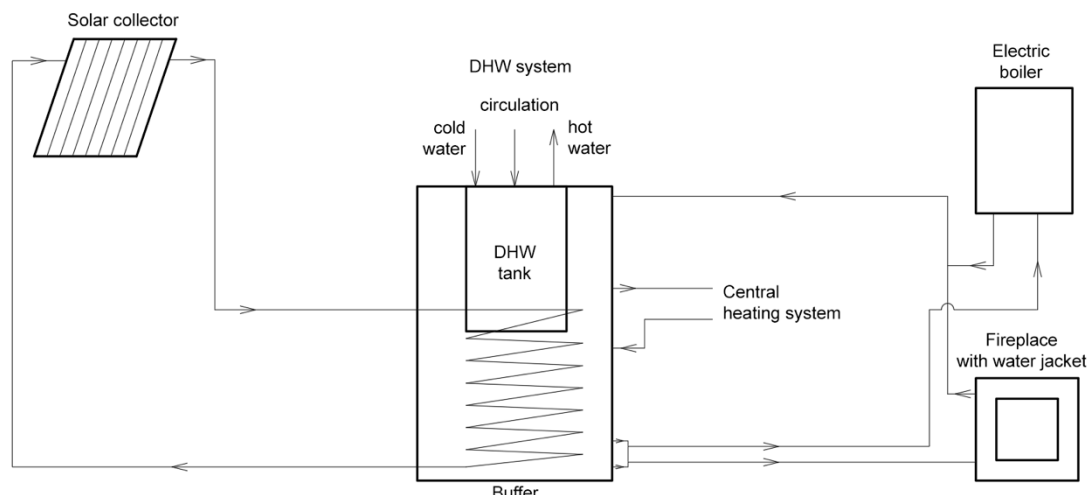


Figure 2. Schematic diagram of the heat source.

2.3. Heating and Domestic Hot Water Systems

The central heating system uses hydronic floor surface heaters divided into two heating circuits: Ground floor and first floor. Nominal operational parameters are 55/45 °C. Mixing systems with three-way valves connected to the weather regulator are used on the branches in the boiler room. Furthermore, room temperature control uses room thermostats. The installation was hydraulically balanced by using balancing valves. The heating system works properly and there are no overheated or under heated rooms in the building.

Cold water is supplied into the building from the backyard well. DHW installation has a circulation pump system that provides hot water as soon as the draw-off valve is opened when the circulation

pump is on and shortly after it has been turned off. The operation cycles of the circulation pump are controlled by a time controller set to start the pump in periods when household members most often use DHW.

2.4. Ventilation System

The house is equipped with a mechanical ventilation system with heat recovery. The ventilation heat recovery (VHR) unit is located in an internal utility room, and ducts run in the space above the ceiling in heated rooms. Table 1 summarizes the technical data of the used VHR unit. Mechanical ventilation nearly covers the whole building. The air is supplied to the rooms located on the ground floor: The living room, the dining room, and the office, and to the rooms on the first floor: Four bedrooms and the recreation room. Exhaust openings are located in two bathrooms, kitchen, and wardrobe. To increase the heat recovery efficiency, a ground plate heat exchanger (GHE) is used to preheat the outside air during the winter. Figure 3 shows the scheme of the ventilation system.

Table 1. Technical data of ventilation heat recovery (VHR) unit.

Operating Mode	Airflow (m ³ /h)	Fan Power (W)
1	350–600	175
2		200
3		235
4		350

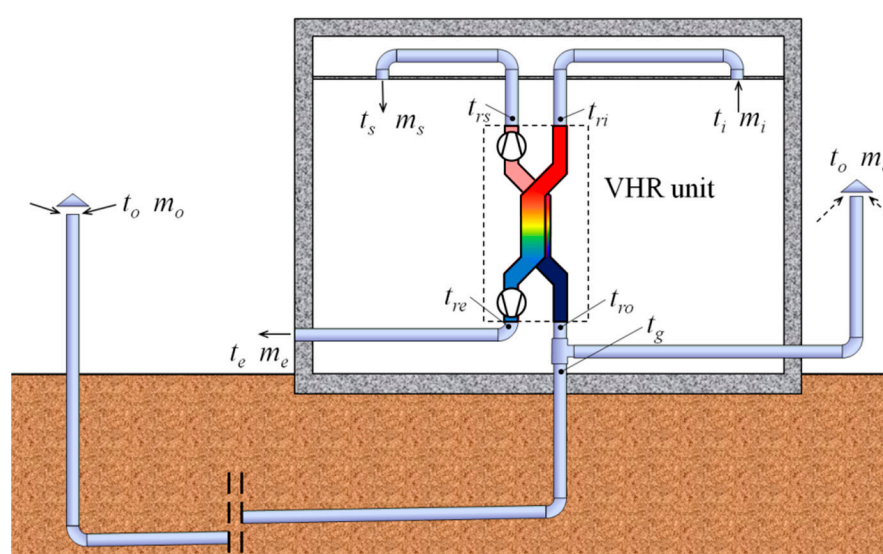


Figure 3. The scheme of the ventilation system, where: t_o -outdoor air temperature, t_g -air temperature at GHE outlet, t_{ro} -outdoor air temperature at VHR unit inlet, t_{rs} -supply air temperature at VHR unit outlet, t_s -supply air temperature, t_i -indoor air temperature, t_{ri} -indoor air temperature at VHR unit inlet, t_{re} -exhaust air temperature at VHR unit outlet, t_e -exhaust air temperature, m_o -outdoor air mass flow rate, m_s -supply air mass flow rate, m_i -indoor air mass flow rate, m_e -exhaust air mass flow rate.

3. Methodology

The comprehensive thermal diagnostics of the building was held from 14 March to 3 April 2012. Throughout the whole measurement period, the outdoor conditions were monitored by the movable meteorological station (CabledVantage Pro2, Davis, CA, USA) placed at the study side. The collected data include dry-bulb outdoor air temperature, relative humidity, wind speed and direction, solar radiation on the horizontal surface, atmospheric pressure, and amount of precipitation.

During the study, we used a wireless measurement system, which has been developed within the research project that the presented work is a part of [18]. The system aims to organize the central database of measurement data collected during the complex thermal diagnostics of the building. It integrates the system instruments with digital outputs, analog voltage/current outputs, and thermal resistor sensors using a wireless data transmission in the ZigBee standard with a local computer.

3.1. Building Envelope

The conducted diagnostics of heat transfer coefficients of external walls based on the available part of the archival project and site studies. It included determination of heat transfer coefficients and thermovision examination of thermal bridges and insulation quality. Calculations of thermal resistance and thermal transmittance followed the procedures set out in the standard [43], which provides the method of calculation of the thermal resistance and thermal transmittance of building components and building elements, excluding doors, windows and other glazed units, curtain walling, components that involve heat transfer to the ground, and components through which air is designed to permeate. The calculation method is based on the appropriate design thermal conductivities or design thermal resistances of the materials and products for the application concerned. The method applies to components and elements consisting of thermally homogeneous layers (which can include air layers).

The thermal transmittance could be calculated by simplified method according to [43]. The principle of the calculation method is as follows: (a) Obtain the thermal resistance of each thermally homogeneous or inhomogeneous part of the building element; (b) combine these individual resistances to obtain the total thermal resistance of the building element, including (where appropriate) the effect of surface resistances; (c) calculate the theoretical heat transfer coefficients for external walls based on Equation (1) taking into account total thermal resistance resulting from resistances of individual materials of the partition:

$$U = \frac{1}{R_T}, \quad (1)$$

where U is thermal transmittance, $W/(m^2 \cdot K)$ and R_T is total thermal resistance of the wall, $(m^2 \cdot K)/W$.

Corrections to the thermal transmittance, as appropriate for the building element concerned, were calculated according to Annex F [43]. Material information for all partition layers was taken in accordance with the manufacturer's data. Detailed description of the calculation methodology of thermal transmittance for external walls is presented in [22].

Direct measurements of heat flux density, temperature difference between indoor and outdoor air (on both side of the partition) were performed using the Testo 435-2 device (Testo, Inc., Lenzkirch, Germany). Outdoor conditions were taken from the meteorological station records. The results were recorded in 1-h intervals. All site studies on building envelope were carried out during the winter. The use of heating system guaranteed the temperature difference between the indoor and outdoor environment at a minimum level of 10 °C, as recommended by [44]. Complementary measurements were made with the thermal imaging camera (FLIR B200, FLIR Systems, Inc., Stillwater, OK, USA).

3.2. Heat Source

The diagnostics of the heat source was carried out when the building was supplied with heat from the electric boiler and solar collectors. Such power supply system enables accurate measurement of energy delivered to the building, using an electricity meter and measuring system in the solar collector system (described below). The efficiency of the fireplace has not been tested because it was not working at the time.

The solar system efficiency was calculated based on the data collected by the meteorological station on 16 March and 23 March. The amount of heat transferred from the solar collectors to the tank was measured using the ultrasonic heat flux meter (SITRANS FUE1010, Siemens AG, Munich, Germany) mounted on the surface of the solar medium return pipe from the water tank (DHW heater), and the set of sensors measuring the temperature and flow of the solar medium from the water tank,

which were connected to the multi-channel recorder (MTT-302, Sensor Electronic, Gliwice, Poland). The values of fluxes of solar radiation on the solar collector plane were determined by “Solar” software based on the measured solar radiation on the horizontal plane.

In order to assess the heat buffer efficiency, we used thermal imaging (CAMERA T335, FLIR Systems, Inc., USA) to determine the distribution of surface temperature at the outer shell of the heat buffer. Based on it, we divided the buffer surface into $j = 5$ zones (from top to bottom). The surface temperature, v_j , was determined for each zone. Moreover, the average indoor air temperature in the boiler room, $t_{i,b}$, was measured.

The theoretical efficiency of solar collector was calculated based on Equation (2):

$$\eta_{T,SC} = \eta_{0,SC} - a_1 \cdot \frac{t_{2,SC} - t_{0,m}}{q_{m,SC}} - a_2 \cdot \frac{(t_{2,SC} - t_{0,m})^2}{q_{m,SC}}, \quad (2)$$

where $q_{m,SC}$ is the average density of solar radiation on the solar collector plane, A_{KS} is the surface area of solar collector, $\eta_{0,SC}$ is the transmission and absorption efficiency of the solar collector, in accordance with the manufacturer's data, $t_{0,m}$ is the average outdoor dry-bulb temperature, $t_{2,SC}$ is the average temperature of the working medium at the solar collector inlet, and a_1 and a_2 are characteristic factors obtained in accordance to the manufacturer's data.

The heat loss from the buffer surface to the environment, Q_A , was calculated according to Equation (3), while Equation (4) was used to determine the efficiency of the heat accumulation in the buffer, $\eta_A(t_i)$.

$$Q_A = \Delta\tau_A \cdot \sum_{j=1}^5 [A_j \cdot h_j \cdot (v_j - t_{i,b})], \quad (3)$$

$$\eta_A(t_i) = 1 - \frac{Q_A}{V_B \cdot c_p \cdot \rho_w \cdot (t_{max} - t_{min})}, \quad (4)$$

where $v_j(\tau)$ is the surface temperature of the outer shell in the j -th zone of the buffer ($^{\circ}\text{C}$), A_j is the surface area of the outer shell in the j -th zone of the buffer (m^2), V_B is the heat buffer capacity, $t_{i,b}$ is the averaged indoor air temperature in the boiler room, h_j is the heat transfer coefficient from the outer shell of the heat buffer, c_p and ρ_w are the specific heat of water and water density for the average buffer water temperature, and t_{max} and t_{min} are the maximum and minimum buffer water temperature.

3.3. Heating and Domestic Hot Water Systems

Transmission efficiency in heating and DHW installations can be calculated in accordance with the procedures set out in the standards [45,46]. Following the procedures, it is necessary to measure the heat loss of installation pipes and define the heat demand for heating and hot water preparation. However, it was not possible to measure the heat loss of the pipes in the tested building, because the heating and hot water pipes run in the wall furrows.

The efficiency of heat emission, including control of the heating installation, is connected to heat transfer losses to the heated room and depends on the type of radiator and the control of the heat emission to the room. It can be determined based on the tables contained in the standard [47] or Regulation [41].

As the building is not connected to the municipal water supply system, the permanent measuring equipment for domestic water installation is not required. For the diagnostics, in order to obtain the value of daily DHW consumption, we recorded the consumption of cold water for 3 weeks (from 14 March to 3 April) with the ultrasound flowmeter (ZDI-05, ALFINE-TIM, Tarnowo Podgórze, Poland).

3.4. Ventilation System

Diagnostics of the ventilation system included tests of: ventilation air distribution, heat recovery efficiency of VHR unit, and heat recovery efficiency of the entire ventilation system.

The measurements of the supply and exhaust airflow rates were performed once at the beginning of the measurement session using the SwemaFlow 233 air capture hood (Swema AB, Sweden). The final result was calculated as an average of 10 single measurements taken in short intervals. We used the BRYMEN BM 157 clamp meter (BRYMEN Technology Corporation, Taiwan) to record the electric power consumed by VHR unit simultaneously with the airflow measurements.

Temperature measurements were carried out for the next 10 days in the period from 25 March to 3 April 2012. The temperature was measured with the 30-channel, precision thermoelectric thermometer type MTT-302 (Sensor Electronic, Poland).

The VHR unit efficiency was calculated from Equation (5):

$$\eta_r = \frac{Q_{rs-ro}}{Q_{ri-ro}} = \frac{m_s c_p (t_{rs} - t_{ro})}{m_e c_p (t_{ri} - t_{ro})}, \quad (5)$$

where Q_{rs-ro} is the heat flux recovered in VHR unit, Q_{ri-ro} is the enthalpy excess of the exhausted air above the enthalpy of air at the inlet of VHR unit, m_s is the supply mass airflow rate, m_e is the exhaust mass airflow rate, c_p is the specific heat at constant pressure, and t_{rs} , t_{ro} , and t_{ri} are according to Figure 3.

Taking into account heat gains/losses in ventilation ducts and GHE, the thermal efficiency of the entire ventilation system was determined from Equation (6):

$$\eta_v = \frac{Q_r}{Q_t} = \frac{m_s c_p (t_s - t_o)}{m_e c_p (t_i - t_o)}, \quad (6)$$

where Q_r is the heat flux transferred to the supplied outdoor air in GHE and VHR unit, Q_t is the excess of enthalpy of the exhaust air above the enthalpy of the outdoor air, c_p is the specific heat at constant pressure, and t_s , t_o , and t_i are according to Figure 3.

3.5. Indoor Environment

The on-site diagnostics of indoor environmental quality was based on the continuous measurements of thermal parameters according to European standards [48,49] and monitoring of the carbon dioxide concentration for assessment of indoor air quality [49] for 3 weeks (14 March to 3 April). Currently, EN 15,251 [49] is superseded by EN 16798-1 [50], in which the major change is splitting up the standard in a normative Part-1 and a Technical Report Part-2. Indoor air temperature (t_a) and relative humidity (RH) were measured with portable loggers (AR235, APAR, Poland) with the accuracy of $\pm 0.5^\circ\text{C}$ and $\pm 3\%$ RH. The CO_2 concentration was monitored in selected rooms with the highest occupancy. The uncertainty of CO_2 monitors was $3\% \pm 10$ ppm (Sensotron, Poland). All measurement instruments fulfilled requirements for accuracy according to EN ISO 7726 [22] and were calibrated before the investigation, and rechecked after the completion of measurements. Room characteristics were used to divide the buildings into homogeneous zones (Figure 4). In each zone, we located at least one sensor (A-APAR, Se-Sensotron). In accordance with this division, appropriate weighting factors for the zone (W_{zone}) and the sensor (W_{sensor}) for the global indoor climate quality evaluation in the building were calculated [25,31]. Indoor environmental quality assessment used categories defined in the standards [49,50], which represent level of occupants expectations with regards to built environment. The categories are as follows: Category I—high level of expectations (associated with spaces for occupants with special needs like children, elderly, etc.), Category II—medium level of expectations (normal level, associated with all new buildings), Category III—moderate level of expectations (associated previously with existing buildings); and Category IV—low level of expectations.

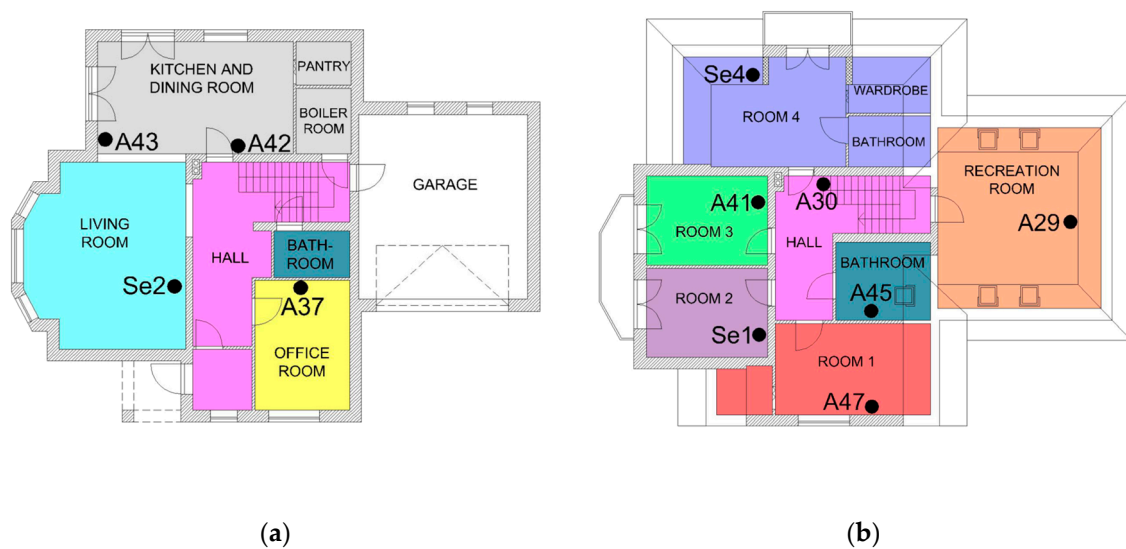


Figure 4. Selection of (a) homogeneous thermal zones on the ground floor and (b) the first floor. Location of loggers is marked with A (APAR, measurements of t_a and RH) and Se (Sensotron, measurements of t_a , RH, and CO₂ concentration).

4. Results

4.1. Building Envelope

Table 2 summarizes the thermal transmittance for the building envelope obtained through calculation methods and from on-site measurements. As it could have been expected, substantial differences are observed. Values of thermal conductivity coefficients adopted for theoretical calculations are often not realistic—especially for insulating materials in existing buildings. Parameters obtained in such manner do not include current features that change over time and due to exposure to moisture.

Table 2. Thermal transmittance of external walls [22].

Wall	Calculated Value, W/(m ² K)	Measured Value, W/(m ² K)
External wall	0.22	0.24
Knee wall	0.30	0.69
Floor on the ground	0.38	-
Floor on the ground-garage	0.60	-
Roof	0.21	0.20
Roof-garage	0.74	-

Window and door joinery thermal insulation information was adopted based on the manufacturer's data. Thermal transmittance values are as follows: 1.8 W/(m² K) for windows in rooms; 2.1 W/(m² K) for roof windows; 2.6 W/(m² K) for glass patio doors; and 2.8 W/(m² K) for the garage door [22]. It was found that all external partitions met the criteria for thermal insulation requirements at that time.

The results of thermovision identification of building envelope are presented in Figures 5 and 6, where thermal bridges are marked with the pink fields. This indicates locally reduced insulation compared to other partitions, which is due to quite common errors made during building construction. Moreover, it affects the real thermal insulation value of the partition.

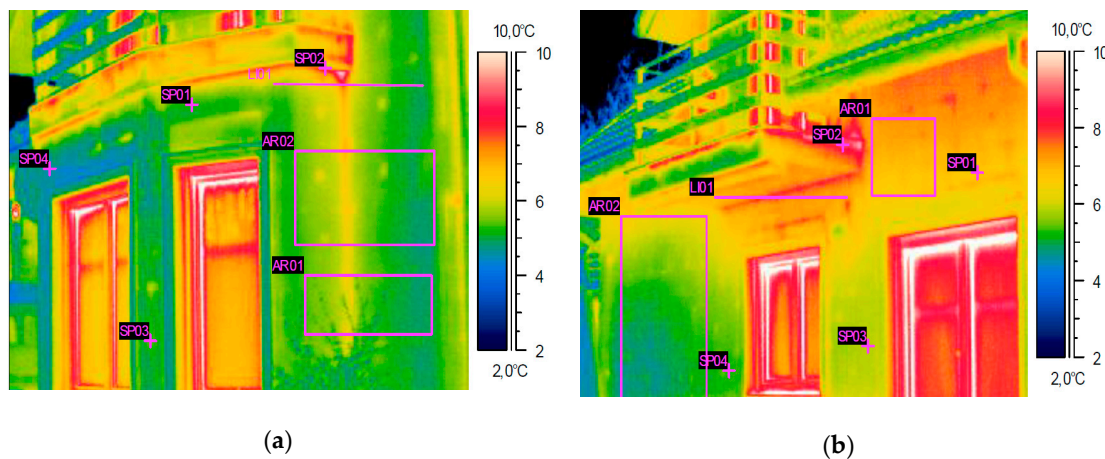


Figure 5. Thermal bridges: (a) Around window openings; (b) Along the length of the balcony panels.

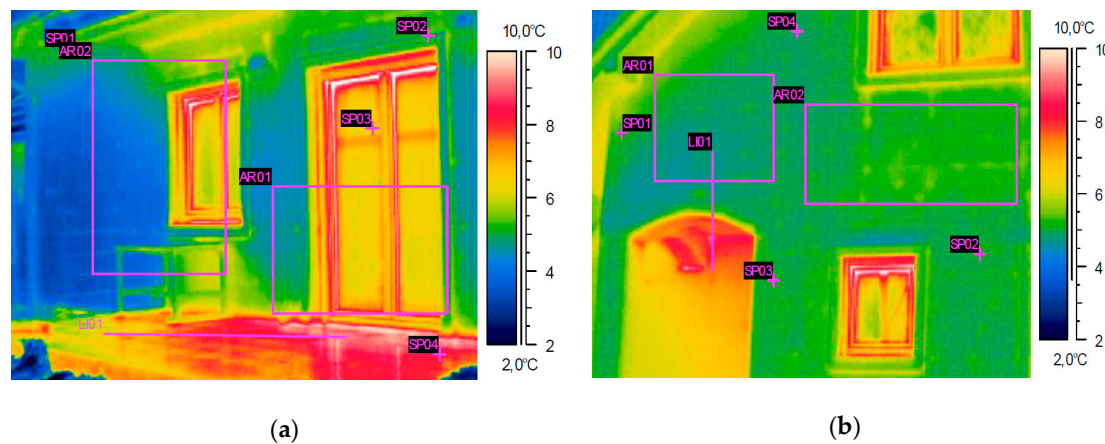


Figure 6. (a) Thermal bridges around patio doors; (b) Leaky insulation surface.

The analysis of identified thermal bridges was carried out using the “KOBRA” electronic thermal bridge catalogue, characterized in [22]. We calculated the following values of linear heat transfer coefficients ψ :

- Around window opening— $\psi = 0.06 \text{ W}/(\text{m}\cdot\text{K})$;
- Along the length of the balcony panels— $\psi = 0.21 \text{ W}/(\text{m}\cdot\text{K})$;
- Around patio doors— $\psi = 0.08 \text{ W}/(\text{m}\cdot\text{K})$.

4.2. Heat Source

4.2.1. Assessment of Solar Collector Efficiency

The theoretical efficiency of solar collector calculated from the Equation (2) equals to $\eta_{T,SC} = 0.74$. This value was obtained from the average measured values ($q_{m,SC} = 800 \text{ W}/\text{m}^2$, $A_{KS} = 3.32 \text{ m}^2$) and data assumed from the manufacturer’s information ($\eta_{0,SC} = 0.85$, $t_{o,m} = 14.8 \text{ }^\circ\text{C}$, $t_{2,S.C} = 38.6 \text{ }^\circ\text{C}$, $a_1 = 2713$, $a_2 = 0.0035$).

Based on the collected data, calculated solar collector efficiency, and performance characteristics of used solar collectors, the annual average transmission efficiency was estimated as 75%, while the annual average operational efficiency of the solar collector was determined to 73%. The total collector efficiency as the source of heat is equal to 0.55 (the product of the determined two efficiencies: 0.75 and 0.73).

4.2.2. Assessment of Heat Buffer Efficiency

We did the calculations for the time of $\Delta\tau_A = 24 \text{ h}$ ($=86,400 \text{ s}$). The values of surface temperature and surface area of the outer shell in each j -th zone of the buffer were obtained from the measurements. Taking measured values as follows: $V_B = 0.55 \text{ m}^3$, $t_{i,b} = 22.1 \text{ }^\circ\text{C}$ and others: $h_j = h = 7 \text{ W}/(\text{m}^2\cdot\text{K})$, $c_p = 4.18 \text{ kJ}/(\text{kg}\cdot\text{K})$, $\rho_w = 985 \text{ kg}/\text{m}^3$, $t_{ma} = 80 \text{ }^\circ\text{C}$, and $t_{min} = 35 \text{ }^\circ\text{C}$ [23], the amount of heat released by buffer from the outer surface during 24 h, calculated from Equation (3), is equal to $Q_A = 3400 \text{ kJ}$, with the accumulation efficiency of $\eta_{A(ti)} = 96.5\%$, as per calculation based on Equation (4).

After taking into account the estimated additional heat losses from the connection stubs, the adjusted accumulation efficiency is 95.6%. Based on the measurement results, the seasonal efficiency of the heat buffer was estimated to be equal to 96%, and the seasonal efficiency of the DHW tank (the tank inside the heat buffer) was determined at 99%.

4.2.3. Assessment of the Electrical Boiler Efficiency and Fireplace with a Water Jacket

The efficiency of electric boilers is close to 100% as they almost have no heat loss. Therefore, the energy efficiency of the electric boiler was estimated to be greater than 99%.

The efficiency of the fireplace with a water jacket (with a built-in heat exchanger) was not investigated and was accepted as 85% according to the tables in the Regulation [41].

4.3. Heating and Domestic Hot Water Systems

Since pipes are installed in wall furrows, we were not able to assess the heat loss within the heating and DHW installations and to determine distribution efficiency through measurements.

The distribution efficiency of floor heating system was estimated at 98% according to the tables in the Regulation [41]. The type of radiators and control system were considered in the assessment of efficiency of emission including control in the heating system. It was estimated as 98% according to the tables in the Regulation [41]. As the hot water intake points are close to the heat source, the distribution efficiency of DHW was estimated at 80% according to the tables in the Regulation [41].

Based on the measurements, the total cold water consumption in this period is 12.4 m^3 , which equals the daily average consumption of $0.59 \text{ m}^3/\text{day}$. Three residents live in the analyzed building. Therefore, the normative water consumption (both cold and hot water) equals to $196.7 \text{ dm}^3/(\text{person}\cdot\text{day})$ [51]. No hot water is used in the analyzed building for washing dishes because occupants installed a dishwasher. Therefore, the share of DHW in total water consumption was estimated at 25%, and the daily DHW consumption was determined at $49.2 \text{ dm}^3/(\text{person}\cdot\text{day})$. Based on the analyses of nonuniformity in water intake during the measuring period, we conclude that it is not possible to reliably assess water consumption based on short-term measurements. One-year monitoring would allow for a more objective assessment of water consumption in the analyzed facility.

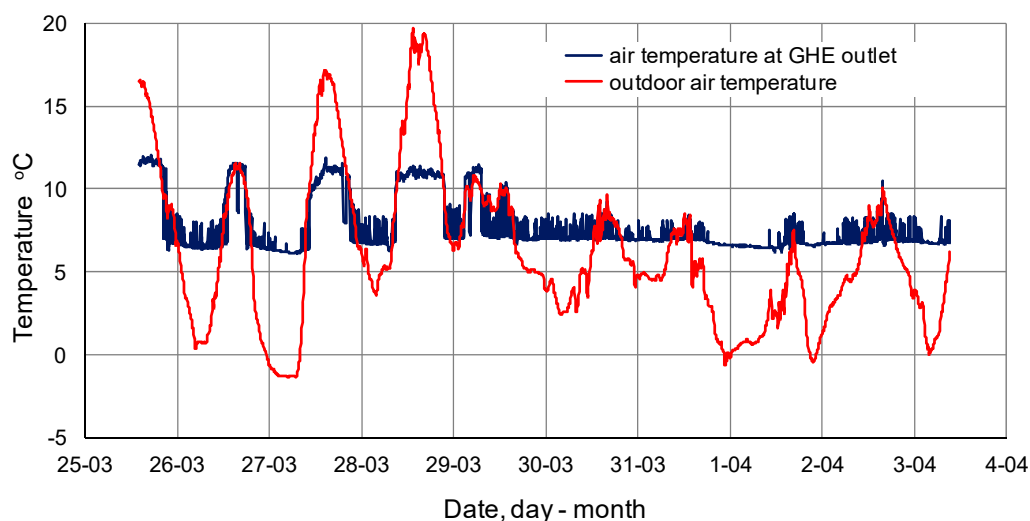
4.4. Ventilation System

The measurement results of ventilation airflow rates are shown in Table 3. The air supply to two unused bedrooms was cut off, while the measured supply airflow in the other two bedrooms was less than the hygienic minimum, i.e., $20 \text{ m}^3/\text{h}/\text{person}$. Total exhaust airflow was slightly lower than the supply one.

Table 3. Ventilation airflow rates—measurement results.

Supply Airflows	Exhaust Airflows
ground floor: living room—58.5 m ³ /h dining room—27.1 m ³ /h office room—17.5 m ³ /h	ground floor: kitchen—65.0 m ³ /h pantry—0.0 m ³ /h bathroom—29.2 m ³ /h
first floor: recreation room—17.0 m ³ /h double bedroom—16.5 m ³ /h single bedroom—8.0 m ³ /h 2 single bedrooms—0.0 m ³ /h sum: 144.6 m ³ /h	first floor: bathroom 1—18.5 m ³ /h bathroom 2—45 m ³ /h wardrobe 1—14 m ³ /h wardrobe 2—0.0 m ³ /h sum: 142.6 m ³ /h

Time series of the outdoor air temperature and the air temperature at the inlet of the VHR unit recorded in the measurement period are shown in Figure 7. The outdoor temperature varied in the large range, from 1.4 °C to 19.7 °C, with an average value of 6.2 °C. The air temperature at the inlet to the VHR unit also showed large fluctuations due to the switching of the damper used to change the inlet of VHR unit from the GHE outlet to the inlet of outdoor air and vice versa. However, in one period from 31 March 18:20 to 1 April 09:20, the outdoor temperature was relatively constant, and the damper position was not changing. Measurement results from this time interval were used to determine the efficiency of VHR unit and for the heat balance of the entire ventilation system. To close this heat balance, the adjustment procedure was applied. Based on the measured volume airflow rates, the supply and exhaust mass airflow rates were estimated and then both airflows were proportionally corrected (by increasing one and reducing the other) so that the heat balance was met. This procedure of adjustment and estimated uncertainties of the measured quantities needed for adjustment are presented in detail in [52].

**Figure 7.** Time series of the outdoor air temperature and the air temperature at the inlet of VHR unit.

Average values of temperature at various points of the ventilation system, supply and exhaust mass airflows, excess of enthalpy at various points of the system, and efficiency of VHR unit and entire ventilation system are presented in Table 4. The heat fluxes in the ventilation system as percentage of enthalpy excess of exhaust air above the outdoor air Q_t are presented in Figure 8. In the selected period, the enthalpy excess of exhaust air above the outdoor air was equal to $Q_t = 934$ W. The enthalpy of supplied outdoor air increased in GHE for $Q_g = 276$ W and in supplied ducts for additional $Q_d = 18$ W. The enthalpy excess of exhaust air above the supplied air at the inlet of VHR unit was equal to $Q_{ri-ro} = 640$ W. In VHR unit, the enthalpy of supplied air increased for $Q_{rs-ro} = 608$ W, which is 95.0% of

$Q_{ri-ro} = 640$ W, ($\eta_r = 95.0\%$). However, it was measured that the electric energy consumption of VHR unit was $Q_e = 182$ W. This energy was used mainly to heat the supplied air. The enthalpy of supplied outdoor air increased in GHE, ducts, VHR unit for $Q_r = Q_g + Q_d + Q_{rs-ro} = 902$ W. Thus, the thermal efficiency of the entire ventilation system defined by Equation (6) was determined at $\eta_v = 96.6\%$.

Table 4. Measurement results from selected period, determined efficiencies of VHR unit and the entire ventilation system, where t_o , t_g , t_{ro} , t_{rs} , t_s , t_{ri} , t_i , t_{re} , and t_e are the temperatures according to Figure 3; m_e and m_s are the mass airflow rates according to Figure 3; Q_g is the increase of supplied outdoor air enthalpy in GHE; Q_d is the increase of air enthalpy in ventilation ducts; Q_e is the electric energy consumption of VHR unit; and Q_r , Q_t , Q_{ri-ro} , Q_{rs-ro} , η_r , and η_v are according to Equations (5) and (6).

Start, 31.03 18:20			Mean \pm SD
End, 01.04:20			
t_o	$^{\circ}\text{C}$	meas.	0.8 ± 0.8
t_g	$^{\circ}\text{C}$	meas.	6.6 ± 0.09
t_{ro}	$^{\circ}\text{C}$	meas.	7.0 ± 0.09
$t_{rs} = t_s$	$^{\circ}\text{C}$	meas.	19.7 ± 0.2
$t_{ri} = t_i$	$^{\circ}\text{C}$	meas.	20.2 ± 0.2
$t_{re} = t_e$	$^{\circ}\text{C}$	meas.	11.3 ± 0.2
m_e	kg/s	meas. & adj.	0.0481
m_s	kg/s	meas. & adj.	0.0477
Q_t	W	-	934
Q_r	W	-	902
Q_g	W	-	276
Q_d	W	-	18
Q_{ri-ro}	W	-	640
Q_e	W	meas.	182
Q_{rs-ro}	W	-	608
η_r	-	Equation (5)	95.0%
η_v	-	Equation (6)	96.6%

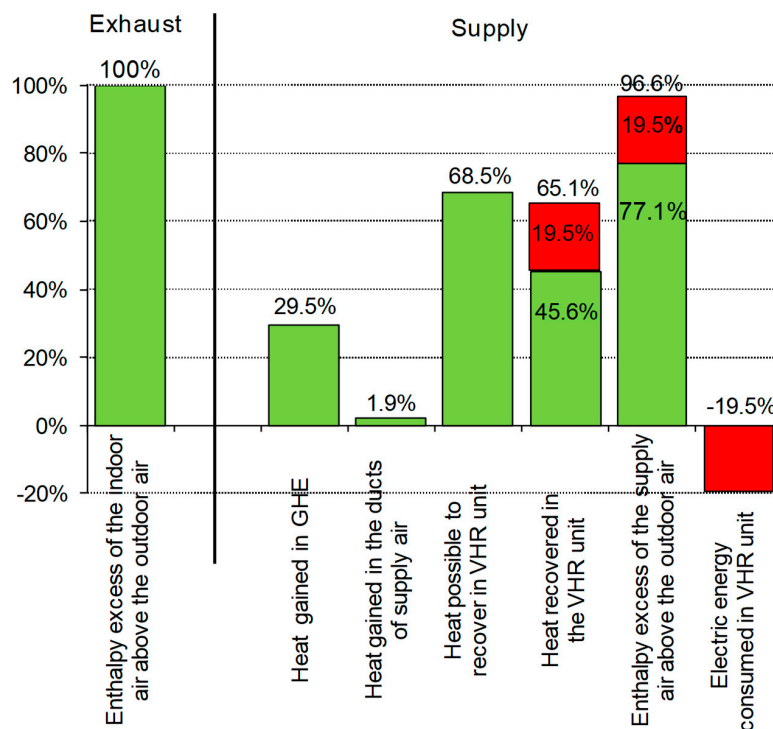


Figure 8. The heat flow balance of ground plate heat exchanger (GHE), VHR unit, and the entire ventilation system.

The ventilation system with GHE and VHR unit operates with high efficiency, above 95%. There are no heat losses from the air ducts—on the contrary, the supplied air is heated in ducts between GHE and VHR unit (1.9%). However, it must be noted that there are some shortcomings of the ventilation system. The disadvantage is the relatively high consumption of the electric energy consumed by the fans and other electrical devices. Most of this energy is contained in the enthalpy of the supply air (up to 19.5%). The distribution of ventilation air in the house is improper as it does not provide the required hygienic airflows to the bedrooms. It could be possible to avoid switching the air dampers at the inlet of the VHR unit by the installation of additional outside air temperature sensor.

4.5. Indoor Environment

Full measurement records have been previously published in paper discussing issues on the assessment of indoor environment diagnostics in residential buildings [31]. Here, we present the summary for the full understanding of the building diagnostic processes by the reader.

Based on the temperature records, we can clearly distinguish zones intended for a frequent occupancy and rooms used occasionally. In the case of rooms used continuously by residents, the air temperature was at the level of 22–25 °C for most of the measurement periods. In rooms used occasionally (i.e., recreation room, wardrobe, guest room, and office), the air temperature oscillated in the range of 19–21 °C for most of the time and reached 22 °C during their use. In all rooms, RH was kept at a moderate level of 30–50% with occasional increases up to 60–70% in the bathroom and wardrobe, which was also used for line drying of clothes.

As residents actively controlled room temperature setpoints accordingly with their needs, the overall thermal environmental quality assessment shows discrepancies between zones. If we focus only on frequently used rooms, the building is characterized with a high quality of the thermal environment. The thermal conditions in those rooms met requirements for the category I 61.1% of the time. Figure 9 shows the overall classification of the thermal environmental quality both for the whole building and taking into account only rooms in permanent use.

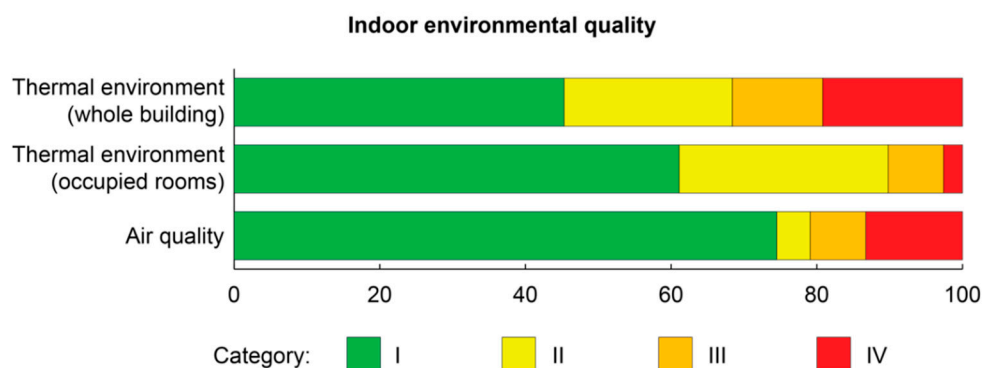


Figure 9. Overall indoor environmental quality assessment based on monitoring. Categorization according to EN 15,251 [49].

The highest concentration of carbon dioxide was registered in bedrooms at nighttime (between 22:00 and 18:00). In one bedroom (Room 2), the CO₂ concentration exceeded the level of 2000 ppm every night. In the second monitored bedroom (Room 1), the CO₂ concentration maintained below 1500 ppm during night time. Such results indicate insufficient ventilation rates in these rooms. The ventilation system diagnostics included spot measurements of airflow rates, which confirmed this indication. The recorded airflow rates were 8 and 16.5 m³/h in Room 2 and Room 1, respectively. The maximum recorded value in the living room is 1085 ppm. In general, the indoor air quality in the studied building was satisfying as it was classified in the I category for most of the time (74.5%, Figure 9).

5. Energy Performance Evaluation of Analyzed Building

Data collected during the energy diagnostics of the building and its installations were applied to determine the energy performance of the object using two methods: First—balance approach based on-site measurements of the heat consumption in the building; and second—computational approach, calculated in accordance with the Regulation [41] with the use both measurement or standard normative data.

The energy performance of the residential building without cooling system includes the components of the heat consumption for the following purposes: Heating and ventilation, domestic hot water, and auxiliary electrical devices. The final energy is calculated taking into account heat demand and efficiencies of DHW, heating, and ventilation systems. The primary energy is determined using non-renewable energy factors.

5.1. The Energy Performance of the Building Determined Based On-Site Measurements of the Heat Consumption in the Building

The heat consumption for heating and ventilation purposes in the standard heating season was calculated using the method based on the heat balance of the building presented in [30]. This method involves the forecasting of the heat consumption for heating and ventilation purposes in the standard heating season based on short-term measurements (lasting minimum 14 days) during the actual season. In this method, the characteristic value for the building—the equivalent thermal resistance for heat losses by transmission and ventilation—is determined from the stationary heat balance (the components of the heat balance are averaged over 14 days). The measured heat flow rates delivered to the building from the heat source are compared to the calculated heat flow rates resulting from the balance (supplied by solar gains through the windows, from the people and equipment, connected to the transmission, and ventilation losses). The characteristic value is determined using the Solver in the Microsoft Excel spreadsheet, by finding the minimum sum of the squared differences between the calculated and measured heat flow rates in 14-days periods. Then, we can evaluate the heat flow rate for heating and ventilation for the standard heating season (for the reference climate) and subsequently seasonal heat consumption (adopting the appropriate length of the heating season). The detailed description of such method can be found in [30].

The measurements of heat consumption were carried out over a period of 19 days (from 15 March to 2 April). The electric boiler and solar collector systems delivered heat for heating and DHW purposes, while the fireplace with a water jacket was turned off. For analyses, we used data obtained from carried out diagnostics as follows: Average hourly values of the outdoor air temperature and total solar radiation on horizontal surface, average daily values of the indoor air temperature in the building, values of ventilation airflow rates, and the efficiencies of heating and DHW systems.

The heat flux (heat power) delivered to the building was measured with the ultrasonic flux meter installed on the surface of the pipeline in the floor heating circuit (in the central heating installation) directly after the heat buffer. The measurements were carried out with the 5 min step and daily averaged. Internal heat gains from people and appliances were estimated based on the measured electricity consumption in the building, the number of residents, and the user behavior survey as well. An average value of internal heat gains of 3.8 W/m^2 was obtained. Heat gains from solar radiation through the windows were calculated in accordance with the standard [53] based on the solar radiation, area, and solar energy transmittance of the glazing. The values of solar radiation falling on individual window orientations were calculated using the TRNSYS simulation program (TYPE 16: Radiation processor) based on measured values of total solar radiation. This module is used to convert solar irradiation on horizontal surface to the oriented and tilted surfaces, in any latitude, based on measured values of the intensity of total irradiation on the horizontal surface.

The forecasted final energy consumption of the examined single-family building for heating and ventilation in the standard heating season for its region is 92 GJ—taking into account the efficiency of the fireplace as a heat source and the efficiency of the heat buffer. This is the heat consumption for

standard outdoor climate conditions and for the actual operational conditions of the building, i.e., the indoor air temperature value of 21.8 °C (the average value from the measurement period), a constant total ventilation airflow rate (Table 3), and internal gains estimated during the measurements.

The final energy consumption for the DHW purposes (for three residents) was calculated in accordance with the guidelines given in the Regulation [41]. Analyses based on the carried out diagnostics: The estimated daily water consumption (49.2 m³/person) and the calculated total efficiency of the DHW system based on the determined component efficiencies (43% with the solar collector system as the heat source and 67% with the fireplace system with a water jacket). It was assumed that 60% of the annual energy for DHW purposes is supplied by the solar installation and 40% by the fireplace.

The final energy consumed by auxiliary electrical devices for heating, ventilation, and hot water preparation was also calculated in accordance to the Regulation [41], based on technical data and the working time of devices.

The final energy indicator EF for heating, ventilation, and hot water preparation (including auxiliary electrical devices) was obtained as 178 kWh/(m² year). In the conducted survey, residents said that the primary source of heating in the examined building was the fireplace with a water jacket, and the electric boiler was used only a few days a year when they are away. We adopted the operating time of the electric boiler as 4% of the heating season duration, while the fireplace was accepted as the heat source in the remaining period. The indicator of non-renewable primary energy EP was determined at 81 kWh/(m² year), assuming the following non-renewable primary energy factors: 0.2 for the fireplace, 3 for electric boiler and auxiliary electrical devices, and 0 for solar collector.

5.2. Computational Energy Performance of the Building

The energy performance of the examined building was calculated in accordance with the Regulation [41]. The methodology of calculations of the energy demand for heating and ventilation purposes included in [41] is based on the heat balance presented in the standard [53]. Calculations are carried out for the normative indoor temperature (i.e., 20 °C) and reference climatic conditions (i.e., monthly outdoor temperatures and radiation to the oriented and tilted surfaces) for the place where building is located. The following data were taken from the thermal diagnostics: Values of thermal transmittances of building partitions and linear heat transfer coefficients of thermal bridges, the average value of internal heat gains, and ventilation airflow rates. In the absence of diagnostic data, we calculated needed values in accordance with the relevant standards or used normative values from the Regulation [41].

As previously, we assumed that 60% of the annual energy for water heating comes from the solar installation and 40% from the fireplace. The operating time of the electric boiler was assumed as 4% of the heating season duration, while the fireplace was accepted as the heat source in the remaining period.

In order to determine the final energy consumption for heating and ventilation purposes, we calculated the total efficiency of heating system based on the component efficiencies from thermal diagnostics (91% with the electrical boiler as the heat source and 78% with the fireplace system with a water jacket).

The final energy consumption for the DHW purposes was calculated in accordance with the guidelines given in the Regulation [41], the same way as described in Section 5.1.

The final energy indicator for heating, ventilation, and DHW purposes was calculated as EF = 113 kWh/(m² year) (including energy consumed by auxiliary electrical devices for heating, ventilation, and hot water preparation, determined the same way as described in Section 5.1).

The indicator of non-renewable primary energy was determined as EP = 57 kWh/(m² year), assuming non-renewable primary energy factors as previously.

6. Conclusions

The energy performance of the building is important in the processes of energy consumption assessment and thermomodernization of buildings as it indicates what elements of the building and installation should be modernized to achieve energy savings. However, the building's energy consumption calculated on the basis of tabular values of the heat balance components, without measurements, is not reliable for such activities. Each building has individual construction and installation solutions. Comprehensive on-site thermal diagnostics provides reliable information about systems and elements and should be the basis for calculations of the energy performance. It is not always possible to measure all the necessary data in a real building, as shown in the article. In such case, it is necessary to use standard normative tabular data. In the described case study, we presented the methodology and results of on-site thermal diagnostics of the single-family house. The results of measurements were used to prepare energy performance of the examined building. We analyzed calculated energy indicators in terms of compliance with Polish requirements for buildings. Moreover, the indoor environmental quality was assessed as satisfying for most of the time.

The indicator of the final energy for heating, ventilation, and DHW purposes of analyzed building obtained using the calculation method ($EF = 113 \text{ kWh}/(\text{m}^2 \text{ year})$) is lower than one obtained using the method based on the measurements ($EF = 178 \text{ kWh}/(\text{m}^2 \text{ year})$). First of all, the reason of the difference is the adoption of the normative indoor air temperature for the calculations (i.e., 20°C) as required by the methodology in the Regulation [41]. In fact, the indoor air temperature maintained in the building during measurements was almost 2°C higher than the normative one. However, if assuming the indoor air temperature equal to the measured values, the final energy indicator is determined at $EF = 127 \text{ kWh}/(\text{m}^2 \text{ year})$ —still lower than that obtained from the method based on measurements. The main reason for such a discrepancy between the obtained values is the fact that the measurements were made at the end of the heating season—in the second half of March when the heat consumption was small due to high insulation of the building. Moreover, studies showed that in March, April, and October, the determination of heat consumption for heating and ventilation based on short-term measurements was burdened with high uncertainty (even up to 50% because of high intensity of solar radiation), while in the remaining months, the uncertainty did not exceed 20% [30].

Indicators of non-renewable primary energy for heating, ventilation, and DHW purposes obtained for both methods (based on measurements— $EP = 81 \text{ kWh}/(\text{m}^2 \text{ year})$, calculations— $EP = 57 \text{ kWh}/(\text{m}^2 \text{ year})$) are lower than the indicator required nowadays in the Polish legislation, which is equal to $EP = 95 \text{ kWh}/(\text{m}^2 \text{ year})$. It turns out that the building built in 2008 meets the requirements that are currently in force in Poland (10 years later) in accordance with the Act [4].

Author Contributions: Literature review, M.K.; methodology, investigation, formal analyses, writing—Original draft, M.H., M.K., A.L., A.P., and A.S.; supervision, writing—Review and editing, Z.P.

Funding: The work was performed within the framework of research task No. 4: “The development of thermal diagnostics of buildings” within the Strategic Research Project funded by the National Centre for Research and Development: “Integrated system for reducing energy consumption in the maintenance of buildings” and Statutory works No. 08/010/BK_17/0024 and 08/010/BK_16/0015, funded by the Ministry of Science and Higher Education.

Conflicts of Interest: The authors declare no conflicts of interest.

References

1. Energy Information Administration (EIA). U.S. Energy Information Administration (EIA). Available online: <https://www.eia.gov/> (accessed on 29 October 2019).
2. European Commission Energy. Available online: <https://ec.europa.eu/energy/en> (accessed on 29 October 2019).
3. European Parliament. Directive 2012/27/EU of the European Parliament and of the Council of 25 October 2012 on Energy Efficiency, Amending Directives 2009/125/EC and 2010/30/EU and Repealing Directives 2004/8/EC and 2006/32/EC. *Off. J. Eur. Union* **2012**, *315*, 1–56.

4. Regulation of the Minister of Infrastructure and Construction of 14 November 2017 Amending the Regulation on the Technical Conditions to be Met by Buildings and Their Location; Journal of Laws 2017, item. 2285; Chancellery of the Prime Minister of Poland: Warsaw, Poland, 2017; Volume Dz.U. 2017.2285.
5. Fleiter, T.; Steinbach, J.; Ragwitz, M.; Reiter, U.; Catenazzi, G.; Jakob, M.; Naegeli, C. Work package 1: Final energy consumption for the year 2012. In *Mapping and Analyses of the Current and Future (2020–2030) Heating/Cooling Fuel Deployment (Fossil/Renewables)*; Fraunhofer and alia for European Commission: Zurich, Switzerland, 2016.
6. Pombo, O.; Allacker, K.; Rivela, B.; Neila, J. Sustainability assessment of energy saving measures: A multi-criteria approach for residential buildings retrofitting—A case study of the Spanish housing stock. *Energy Build.* **2016**, *116*, 384–394. [[CrossRef](#)]
7. Picallo-Perez, A.; Sala-Lizarraga, J.M.; Iribar-Solabarrieta, E.; Odriozola-Maritorenna, M.; Portillo-Valdés, L. Application of the malfunction thermoeconomic diagnosis to a dynamic heating and DHW facility for fault detection. *Energy Build.* **2017**, *135*, 385–397. [[CrossRef](#)]
8. Pardo, N.; Thiel, C. Evaluation of several measures to improve the energy efficiency and CO₂ emission in the European single-family houses. *Energy Build.* **2012**, *49*, 619–630. [[CrossRef](#)]
9. Jermyn, D.; Richman, R. A process for developing deep energy retrofit strategies for single-family housing typologies: Three Toronto case studies. *Energy Build.* **2016**, *116*, 522–534. [[CrossRef](#)]
10. Pellegrino, M.; Simonetti, M.; Chiesa, G. Reducing thermal discomfort and energy consumption of Indian residential buildings: Model validation by in-field measurements and simulation of low-cost interventions. *Energy Build.* **2016**, *113*, 145–158. [[CrossRef](#)]
11. Christensen, J.E.; Chasapis, K.; Gazovic, L.; Kolarik, J. Indoor Environment and Energy Consumption Optimization Using Field Measurements and Building Energy Simulation. *Energy Procedia* **2015**, *78*, 2118–2123. [[CrossRef](#)]
12. Ma, Z.; Cooper, P.; Daly, D.; Ledo, L. Existing building retrofits: Methodology and state-of-the-art. *Energy Build.* **2012**, *55*, 889–902. [[CrossRef](#)]
13. Audenaert, A.; Briffaerts, K.; Engels, L. Practical versus theoretical domestic energy consumption for space heating. *Energy Policy* **2011**, *39*, 5219–5227. [[CrossRef](#)]
14. Energy in Buildings and Communities Programme (EBC). *EBC Annex 58—Reliable Building Energy Performance Characterisation Based on Full Scale Dynamic Measurements*; International Energy Agency (IEA): Paris, France, 2012.
15. Harrestrup, M.; Svendsen, S. Full-scale test of an old heritage multi-storey building undergoing energy retrofitting with focus on internal insulation and moisture. *Build. Environ.* **2015**, *85*, 123–133. [[CrossRef](#)]
16. Albatayneh, A.; Alterman, D.; Page, A.; Moghtaderi, B. Development of a new metric to characterise the buildings thermal performance in a temperate climate. *Energy Sustain. Dev.* **2019**, *51*, 1–12. [[CrossRef](#)]
17. Harkouss, F.; Fardoun, F.; Biwale, P.H. Optimal design of renewable energy solution sets for net zero energy buildings. *Energy* **2019**, *179*, 1155–1175. [[CrossRef](#)]
18. Hurnik, M.; Specjal, A.; Popiolek, Z.; Kierat, W. Assessment of single-family house thermal renovation based on comprehensive on-site diagnostics. *Energy Build.* **2018**, *158*, 162–171. [[CrossRef](#)]
19. López-González, L.M.; López-Ochoa, L.M.; Las-Heras-Casas, J.; García-Lozano, C. Final and primary energy consumption of the residential sector in Spain and La Rioja (1991–2013), verifying the degree of compliance with the European 2020 goals by means of energy indicators. *Renew. Sustain. Energy Rev.* **2018**, *81*, 2358–2370. [[CrossRef](#)]
20. Csoknyai, T.; Legardeur, J.; Akle, A.A.; Horváth, M. Analysis of energy consumption profiles in residential buildings and impact assessment of a serious game on occupants' behavior. *Energy Build.* **2019**, *196*, 1–20. [[CrossRef](#)]
21. Zhao, X.; Li, N.; Ma, C. Residential energy consumption in urban China: A decomposition analysis. *Energy Policy* **2012**, *41*, 644–653. [[CrossRef](#)]
22. Steidl, T. (Ed.) Diagnostyka in situ Izolacyjności Ciepłej Budynków (On-Site Diagnostics of Building Thermal Insulation). In *Guide to Thermal Diagnostics of Buildings*; Poradnik diagnostyki ciepłej budynków; Wydział Inżynierii Środowiska i Energetyki, Politechnika Śląska: Gliwice, Poland, 2013; Volume 1, ISBN 978-83-936995.

23. Foit, H. (Ed.) Diagnostyka in situ Źródeł Ciepła Oraz Instalacji Grzewczych i Ciepłej Wody Użytkowej (On-Site Diagnostics of Heat Sources and Heating and Domestic Hot Water Installations). In *Guide to Thermal Diagnostics of Buildings*; Poradnik diagnostyki cieplnej budynków; Wydział Inżynierii Środowiska i Energetyki, Politechnika Śląska: Gliwice, Poland, 2013; Volume 2, ISBN 978-83-936995-2-0.
24. Trzeciakiewicz, Z. (Ed.) Diagnostyka in situ Źródeł Chłodu Oraz Instalacji Wentylacyjnych i Klimatyzacyjnych (On-Site Diagnostics of Cooling Sources, Ventilation and Air Conditioning Systems). In *Guide to Thermal Diagnostics of Buildings*; Poradnik diagnostyki cieplnej budynków; Wydział Inżynierii Środowiska i Energetyki, Politechnika Śląska: Gliwice, Poland, 2013; Volume 3, ISBN 978-83-936995-3-7.
25. Kaczmarczyk, J. (Ed.) Diagnostyka in situ Środowiska Wewnętrznego w Budynkach (On-Site Diagnostics of Indoor Environment in Buildings). In *Guide to Thermal Diagnostics of Buildings*; Poradnik diagnostyki cieplnej budynków; Wydział Inżynierii Środowiska i Energetyki, Politechnika Śląska: Gliwice, Poland, 2013; Volume 4, ISBN 978-83-936995-4-4.
26. Popiolek, Z. (Ed.) Kompleksowa Diagnostyka Ciepła Budynków in situ w Praktyce (Comprehensive On-Site Thermal Diagnostics of Buildings in Practice). In *Guide to Thermal Diagnostics of Buildings*; Poradnik diagnostyki cieplnej budynków; Wydział Inżynierii Środowiska i Energetyki, Politechnika Śląska: Gliwice, Poland, 2013; Volume 5, ISBN 978-83-936995-4-1.
27. Specjał, A. (Ed.) Metodyka Wyznaczania Świadczenia Charakterystyki Energetycznej Budynku na Podstawie Pomiarów (Method for Drawing up a Building Energy Performance Certificate Based on the Measurements). In *Guide to Thermal Diagnostics of Buildings*; Poradnik diagnostyki cieplnej budynków; Wydział Inżynierii Środowiska i Energetyki, Politechnika Śląska: Gliwice, Poland, 2013; Volume 6, ISBN 978-83-936995-6-8.
28. Ferdyn-Grygierek, J.; Bartosz, D.; Specjał, A.; Grygierek, K. Analysis of Accuracy Determination of the Seasonal Heat Demand in Buildings Based on Short Measurement Periods. *Energies* **2018**, *11*, 2734. [[CrossRef](#)]
29. Specjał, A. Dokładność wyznaczania charakterystyki energetycznej budynków na podstawie krótkich pomiarów. *Rynek Energii* **2012**, *6*, 63–69.
30. Specjał, A.; Bartosz, D. Determination of the seasonal heat consumption based on the short-term measurements in the building. *J. Build. Phys.* **2017**, *40*, 544–560. [[CrossRef](#)]
31. Kaczmarczyk, J.; Lipczyńska, A.; Kateusz, P. Indoor environmental quality evaluation in dwellings: A Polish case study. *ACEE Archit. Civ. Eng. Environ.* **2017**, *10*, 163–171.
32. Kaczmarczyk, J.; Ferdyn-Grygierek, J.; Baranowski, A. The impact of building parameters and way of operation on the operative temperature in rooms. *ACEE Archit. Civ. Eng. Environ.* **2018**, *11*, 107–114. [[CrossRef](#)]
33. Jakubiec, J.; Żurkowski, R. Wielozadaniowy system operacyjny komunikatora systemu diagnostyki cieplnej budynków (The multitasking operating system for a communicator in a building thermal diagnostic system). *Pomiary Autom. Kontrola* **2014**, *60*, 228–232. (In Polish)
34. Bartosz, D. Wpływ stanu ochrony cieplnej budynku na dokładność wyznaczania sezonowego zużycia ciepła metodą regresji (The impact of the energy quality of the building on the seasonal heat demand determination accuracy using the energy signature method). *Rynek Energii* **2013**, *3*, 121–129. (In Polish)
35. Popiolek, Z.; Kateusz, P. Comprehensive thermal diagnostics on-site of buildings. *ACEE Archit. Civ. Eng. Environ.* **2017**, *10*, 125–132.
36. Blaszczyk, M.; Król, M.; Hurnik, M. On-site diagnostics of mechanical ventilation systems in office buildings. *ACEE Archit. Civ. Eng. Environ.* **2017**, *10*, 145–156.
37. Hurnik, M.; Blaszczyk, M.; Król, M. On-site thermal diagnostics of cooling sources for air conditioning systems in office buildings. *ACEE Archit. Civ. Eng. Environ.* **2017**, *10*, 157–163. [[CrossRef](#)]
38. Bartosz, D.; Specjał, A. Estimation of the seasonal demand for cooling based on the short-term data. *ACEE Archit. Civ. Eng. Environ.* **2017**, *10*, 133–143. [[CrossRef](#)]
39. Bartosz, D. Comprehensive energy diagnostics carried out in a residential building—A case study. *ACEE Archit. Civ. Eng. Environ.* **2018**, *11*, 137–150. [[CrossRef](#)]
40. Specjał, A.; Ciuman, H. On-site thermal diagnostics of heating and DHW installations. *ACEE Archit. Civ. Eng. Environ.* **2017**, *10*, 165–173. [[CrossRef](#)]
41. Regulation of the Minister of Infrastructure and Development of 27 February 2015 on the Methodology for Calculating the Energy Performance of a Building or Part of a Building and Energy Performance Certificates; Journal of Laws 2015, item. 376; Chancellery of the Prime Minister of Poland: Warsaw, Poland, 2015; Volume 376.

42. Peel, M.C.; Finlayson, B.L.; McMahon, T.A. Updated world map of the Köppen-Geiger climate classification. *Hydrol. Earth Syst. Sci. Discuss.* **2007**, *4*, 439–473. [[CrossRef](#)]
43. EN ISO 6946. *Building Components and Building Elements—Thermal Resistance and Thermal Transmittance—Calculation Methods*; European Committee for Standardization: Brussels, Belgium, 2007.
44. ISO 9869. *Thermal Insulation—Building Elements—In-Situ Measurement of Thermal Resistance and Thermal Transmittance (REVISED BY ISO 9869-1:2014)*; International Organization for Standardization (ISO): Geneva, Switzerland, 2014.
45. EN 15316-2-3. *Heating Systems in Buildings. Method for Calculation of System Energy Requirements and System Efficiencies. Part 2-3: Space Heating Distribution Systems*; European Committee for Standardization: Brussels, Belgium, 2007.
46. EN 15316-3-2. *Heating Systems in Buildings. Method for Calculation of System Energy Requirements and System Efficiencies. Part 3-2: Domestic Hot Water Systems, Distribution*; European Committee for Standardization: Brussels, Belgium, 2007.
47. EN 15316-2-1. *Heating Systems in Buildings. Method for Calculation of System Energy Requirements and System Efficiencies. Part 2-1: Space Heating Emission Systems*; European Committee for Standardization: Brussels, Belgium, 2007.
48. EN ISO 7730. *Ergonomics of the Thermal Environment—Analytical Determination and Interpretation of Thermal Comfort Using Calculation of the PMV and PPD Indices and Local Thermal Comfort Criteria*; European Committee for Standardization: Brussels, Belgium, 2005.
49. EN 15251. *Indoor Environmental Input Parameters for Design and Assessment of Energy Performance of Buildings Addressing Indoor Air Quality, Thermal Environment, Lighting and Acoustics*; European Committee for Standardization: Brussels, Belgium, 2007.
50. EN 16798-1. *Energy Performance of Buildings—Ventilation for Buildings—Part 1: Indoor Environmental Input Parameters for Design and Assessment of Energy Performance of Buildings Addressing Indoor Air Quality, Thermal Environment, Lighting and Acoustics—Module M1-6*; European Committee for Standardization: Brussels, Belgium, 2019.
51. *Regulation of the Minister of Infrastructure of 14 January 2002 on the Determination of Average Standards for Water Consumption*; Journal of Laws 2002, no. 8, item. 70; Chancellery of the Prime Minister of Poland: Warsaw, Poland, 2002; Volume Dz.U.2002 nr 8 poz. 70.
52. Hurnik, M.; Specjal, A.; Popiolek, Z. On-site diagnosis of hybrid ventilation system in a renovated single-family house. *Energy Build.* **2017**, *149*, 123–132. [[CrossRef](#)]
53. EN ISO 13790. *Energy Performance of Buildings—Calculation of Energy Use for Space Heating and Cooling*; European Committee for Standardization: Brussels, Belgium, 2008.



© 2019 by the authors. Licensee MDPI, Basel, Switzerland. This article is an open access article distributed under the terms and conditions of the Creative Commons Attribution (CC BY) license (<http://creativecommons.org/licenses/by/4.0/>).